IL NUOVO CIMENTO **47 C** (2024) 258
DOI 10.1393/ncc/i2024-24258-9

Communications: SIF Congress 2023

Optical calibration of standing wave acoustic levitator

S. Marrara([1])([2])

([1]) *Dipartimento MIFT, Università degli Studi di Messina - V.le F. Stagno d'Alcontres 31, 98166 Messina, Italy*
([2]) *IPCF-CNR - V.le F. Stagno d'Alcontres 37, 98158 Messina, Italy*

received 30 January 2024

Summary. — Acoustic tweezers are devices that use acoustic radiation forces to counteract gravity and trap and maneuver objects in air, liquids, or gases, without touching them or contaminating the sample. This article will explain what acoustic trapping is, the theory behind it and the calibration techniques used to study the acoustic forces acting on particles trapped in phased array levitators, focusing on the calibration of TinyLev acoustic levitator. The reported methods allows us to calculate the force constants of the trap, giving the opportunity to make use of these tools for several applications, from biomedical to chemico-physical fields.

1. – Introduction

The term levitation derives from the Latin "levitas", which means "lightness". In fact, levitation refers to the process of an object overcoming the force of gravity and remaining suspended in a fluid. Often this term, used in a paranormal or metaphysical context, describes an object that seems to rise into the air on its own: this is somewhat the effect obtained by seeing the levitation of particles of different nature without touching them. From here we understand well how levitating an object without touching it can be fundamental in the scientific field, in many sectors ranging from medicine to physics. For example, levitation could be used in astrophysics to study extraterrestrial particles such as meteorites, star dust, but it is also important in the medical field for transporting medicines into the body or for removing bacteria. Thanks to the progress made in recent years, what has just been said is not just something metaphysical or an idea, but it is reality. It is possible to levitate particles of different nature by using tools called "tweezers", precisely because they allow particles to be trapped, moved and manipulated. Among these, the best known levitations are magnetic [1], optical [2], electrostatic [3] and acoustic [4]. This article will be devoted to acoustic levitation and its use by means of the phased array levitators. Acoustic Tweezers (ATs) use acoustic waves to manipulate microscopic objects precisely, selectively and without contact. This allows to move small solid or liquid objects in the air by exploiting the pressure generated by sound waves that overcome the force of gravity. "Phased Array" (PAL) levitators allow acoustic levitation to be achieved by using an array of low-cost transducers to generate a complex acoustic pressure field to levitate and manipulate an object. Their main feature is low energy consumption. The first of these type of levitators was a single-axis standing wave levitator called TinyLev [5, 6]. Today acoustic trapping can be used not only to levitate objects larger than the acoustic wavelength produced, but also to rotate them. Acoustic tweezers technology, therefore, allows particles of various physical properties to be manipulated without causing damage to samples [7]. Thus, the wide range of acoustic frequencies allows acoustic tweezers to manipulate particles ranging in size from nanometers to millimeters [8]. These characteristics have made acoustic tweezers useful enough to be used in numerous applications from biomedical to chemico-physical fields.

In sect. **2**, we briefly describe the theoretical background of acoustic trapping and the theory used in this work. A brief description of the phased array levitator used —the TinyLev— and its calibration to calculate force constants using video microscopy and a four-quadrant detector in sect. **3**. In sect. **4**, the experimental results, future perspectives and conclusions will be illustrated.

2. – Theory

Generally, realizing an acoustic trap is equal to model transducers as circular pistons whose far-field acoustic pressure is compared with the acoustic pressure of our transducers [9]. When a particle is suspended in the field of a sound wave, an acoustic radiation force is exerted on the particle [10]. Acoustic radiation forces originate from the diffusion and absorption of acoustic waves, and depend on gradient and diffusion forces —similarly to what happens in the case of optical trapping. The theory underlying acoustic radiation forces is studied by considering the dispersion and absorption of acoustic waves through the Navier-Stokes equations for fluid mechanics [11]. The acoustic force acting on a particle is expressed as

$$\mathbf{F}_{ac} = \mathbf{F}_{grad} + \mathbf{F}_{scat} + \mathbf{F}_{abs} + \mathbf{F}_{str}. \tag{1}$$

Thus, the particle experiences not only radiation force components due to pressure gradients ($\mathbf{F}_{grad}$) scattering ($\mathbf{F}_{scat}$) and absorption within the particle ($\mathbf{F}_{abs}$), but also drag forces due to streaming ($\mathbf{F}_{str}$). Assuming we are dealing with a spherical particle, in the regime where the particle size is significantly smaller than the acoustic wavelength in the fluid, we can apply the Gor'kov potential theory. Through this theory it is possible to calculate the gradient force (predominant compared to the others reported in the equation above) which turns out to be the main force from which the trapping phenomenon derives

$$\mathbf{F} = -\nabla U, \tag{2}$$

where the Gor'kov potential U is

$$U = \frac{1}{4} V \left(\frac{1}{c_0^2 \rho_0} - \frac{1}{c_p^2 \rho_p} \right) (|P|^2) - \frac{3}{4} V \left(\frac{\rho_p - \rho_0}{\omega^2 \rho_0 (\rho_0 + 2\rho_p)} \right) \left(\left| \frac{\partial P}{\partial x} \right|^2 + \left| \frac{\partial P}{\partial y} \right|^2 + \left| \frac{\partial P}{\partial z} \right|^2 \right). \tag{3}$$

In eq. (3), V is the volume of the particle, c_0 and c_p are the speed of sound in the medium and the particle, respectively, ρ_0 and ρ_p are the densities of the medium and of the particle, and ω is the angular frequency of the emitted waves.

Unifying the theoretical approach with a simulative one, it would be possible to make use of this equation to determine the force constants and verify if and how good they coincide with the experimental ones, as shown in [9]. Instead, in this paper the potential was modeled in a simpler way than the Gor'kov potential by referring to the characteristic potential of a harmonic oscillator.

Consequently, we have

$$\begin{cases} F_x \approx -k_x x \\ F_y \approx -k_y y \\ F_z \approx -k_z z, \end{cases} \tag{4}$$

where k_x, k_y and k_z are the force constants of the trap along x, y and z, respectively. The values of these terms will be calculated by the calibration methods, as shown in the following sections.

3. – Materials and methods

Acoustic trapping measurements were performed by means of the TinyLev levitator, made up of 72 transducers with a diameter of 10 mm. Every transducer emits ultrasound at 40 kHz and they are arranged half in the upper matrix and half in the lower one of the apparatus, respectively. The acoustic waves that propagate in the air at that frequency are characterized by having a wavelength of 8.65 mm at 25 °C and allow the levitation of samples up to 4 mm (half a wavelength). As regards the distance between the two arrays, it was seen that it influences the capture force of the device. as the distance between the two surfaces increases, the radius of curvature of the same also increases. The z force directed longitudinally with respect to the levitated body must be as high as possible, in order to counteract gravity and ensure levitation; the lateral forces x and y may be smaller, but are still important to provide stability to the levitated object [5]. The transducers are controlled by a system appropriately programmed on the Arduino Nano board, which generates two guide signals to produce the vertical movement of the traps. In the tweezers there are a knob or three buttons through which it is possible to vary the phase of the two arrays, allowing the trapped particles to rise, fall and return to the central position. It is also possible to trap more particles along the nodes in fig. 1 as the stationary ultrasonic waves produced have defined nodes. A node is the area of minimum pressure, while an antinode is defined as the area of maximum pressure. The circuit is powered via a DC power supply, using a voltage that varies with the sample to be trapped. This longitudinal ultrasound pressure wave allows the particle to hover without contact in the air.

Calibrating the ATs is essential to evaluate the correct functioning of the trap and to study the force that traps the particles. The calibration of TinyLev was performed by using a polystyrene sphere with a diameter of about 1 mm and by means of two different calibration methodologies employing i) video microscopy, and ii) a four-quadrant photodetector (QPD), sensitive to the position of the particle and therefore useful for tracking the fluctuations from the equilibrium position of the acoustically trapped particles [9]. Note that both techniques are used to have a comparison between the results

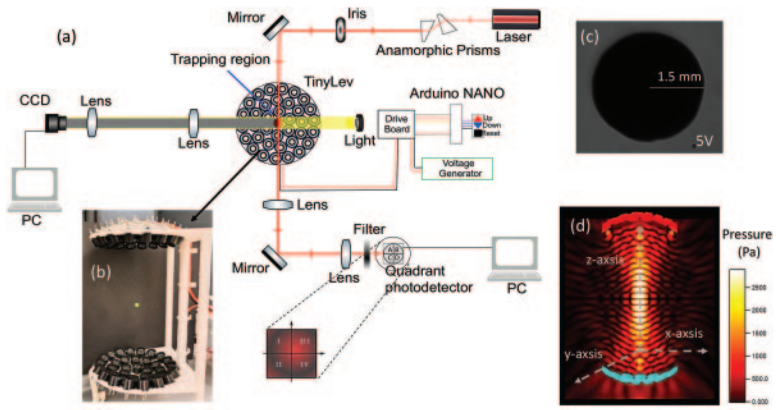

Fig. 1. – (a) Diagram of the experimental apparatus, for simplicity of the tweezers only the lower array has been represented; (b) acoustic tweezers used to carry out calibration measurements. It is made up of 36 transducers in the upper part and 36 in the lower part, each of them emits with a power of 40 KHz; (c) CCD shadow image of a trapped polystyrene sphere; (d) map of the pressure field (in Pa) obtained by software. The trap reference frame is also represented.

obtained, demonstrating the validity of the measurements. A scheme of the experimental setup used is shown in fig. 1(a).

In the same figure is showed that the optical path of our apparatus in video microscopy consists of two lenses in a 2:1 telescope configuration and a CCD camera (BASLER a2A1920-160umPRO). A lamp provides back-lighting of the levitated particle, so that the shadow of the particle is reproduced by the CCD as shown in fig. 1(b). Here is shown a frame of the shadow of a polystyrene ball of radius 1.5 mm and trapped with a voltage of 5 V. A map of the pressure field used is shown in fig. 1(c). Particle tracking is achieved with homemade Python-based codes, which provide the trajectory of the particle center along the transversal x and axial z directions and the average particle radius R by approximating a spherical shape to our particle. While for the method involving the use of the QPD, a diode laser (785 nm), whose beam is made circular by a pair of anamorphic prisms, is directed towards the levitated sphere using ultrasound. The shadow of the trapped particle is imaged through a mirror and two lenses forming a 3:1 telescope configuration and lands on a four-quadrant photodetector (QPD) that records fluctuations in the particle's position along y and z. The voltage signal acquired by the QPD is analyzed by LabView and both the data obtained from the CCD video processing and from the QPD are processed using codes written in Python to obtain the Power Spectrum (PS) that allow us to visualize characteristic peaks in this spectrum due to periodic oscillations of the trapped particle [12].

4. – Discussion and conclusions

Figure 2 reports the PS calculated by tracing the trajectory of a trapped polystyrene ball of approximately 1.5 mm radius. In fig. 2(a), the PS (V^2 s) obtained by analyzing the data acquired from the QPD shows the peaks along y and along z in light blue and in blue, respectively. Figure 2(b) shows the PS obtained from the CCD video data where the PS (pixel^2 s) is represented as a function of the frequencies (Hz). In this case, the peak along x and the one along z are represented in purple and in blue, respectively. Since our setup

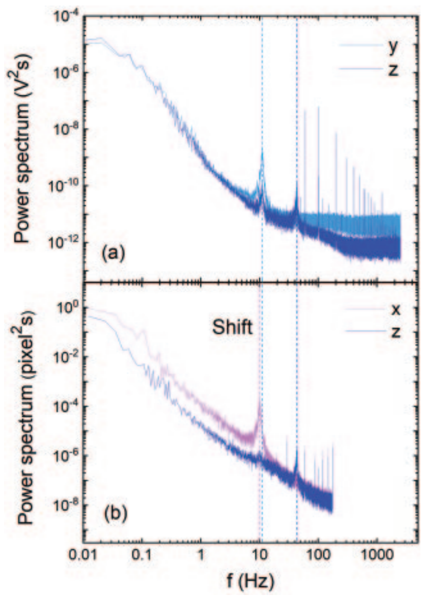

Fig. 2. – Power spectra (PS) of the spontaneous oscillations of a levitated particle along the reference system of the xyz trap. (a) PS of the signal recorded with QPD and (b) PS of the signal recorded with the video camera. The data is displayed both in the original unit (V2s in the QPD case and pixel2s in the CCD case). The dotted lines highlight the correspondence between similar peaks. As you can see the x peak of the CCD and the y peak of the QPD are slightly shifted as highlighted by the purple dotted line, this is due to the imperfect symmetry of the trap.

is built with the upper and lower array in a symmetrical configuration, we should have the same oscillations recorded along x and y, but, comparing figs. 2(a) and (b), the two methodologies coincide along the axial direction z, while there is a slight movement along the transversal x and y directions probably caused by the fact that the two arrays were not mounted in a perfectly symmetrical way. This is highlighted by the measurements carried out. The frequencies at which the peaks are found are approximately $f_x(\text{CCD}) = 10.3\,\text{Hz}$, $f_y(\text{QPD}) = 11.3\,\text{Hz}$ and $f_z(\text{CCD-QPD}) = 44.1\,\text{Hz}$. Knowing the values of these peaks, the density —which is approximately $\rho = 36 \pm 6\,\text{kg/m}^3$— and the radius of our sphere, we can calculate the elastic constants that characterize our trap. In this frame, considering a simple harmonic oscillator model —$f = \frac{1}{2\pi}\sqrt{\frac{k}{m}}$— the elastic constants $k_x(\text{CCD}) = (0.27 \pm 0.05) \times 10^2\,\text{N/m}$, $k_y(\text{QPD}) = (0.23 \pm 0.04) \times 10^2\,\text{N/m}$ and $k_z = (4.24 \pm 0.01) \times 10^2\,\text{N/m}$ are obtained. As you can see we have a higher trapping force along z as the acoustic force is stronger along the longitudinal axis unlike the holographic acoustic tweezers, where the force was stronger along x [9]. In the case of the QPD detector the y peak is also observed in the z power spectrum, probably due to a small asymmetry of the sphere, which induces a tilt on the particle fluctuations [13] between the QPD channels. Note that this effect could also arise in the case of construction defects in the setup, whereby the transducers, not being perfectly aligned, could generate an acoustic field deviated by a small angle along the axis of the tweezers, compared to what is expected. A similar effect is not observed in the signals obtained from the CCD device, because the tracking software fits a circle to the particle image, and therefore, a possible asymmetry of the particles cannot influence the reconstruction of the particle trajectory, as in the QPD case. Due to the limited sampling rate of CCD (352 fps) compared to the one of QPD (5 kHz), the PS calculated with CCD signals are in a shorter frequency range. Anyway, the results of the two methodologies coincide jointly with the fact that the trap is effectively stable even for particles of different shape and nature. This gives us the possibility of measuring acoustic forces acting on the trapped particles either with one configuration —depending on the trapped particles that may be disturbed by the presence of the QPD laser, the available instruments and the laboratory spaces—, or using both the methodologies in combination for a comparison of the results. In this way we can use the acoustic tweezers for several types of applications and studies. A possible development of this work will be to characterize the trapped particles using spectroscopic techniques. However, the path already undertaken has already proven very promising, bringing results not yet achieved with other types of trapping studies.

REFERENCES

[1] Neuman K. C. and Nagy A., *Nat. Methods*, **5** (2008) 491.
[2] Volpe G. *et al.*, *J. Phys. Photon.*, **5** (2023) 022501.
[3] Gerspach M. A. *et al.*, *Microsyst. Nanoeng.*, **3** (2017) 1.
[4] Brandt E. H., *Nature*, **413** (2001) 474.
[5] Marzo A. *et al.*, *Rev. Sci. Instrum.*, **88** (2017) 085105.
[6] Marzo A., `https://www.instructables.com/id/Acoustic-Levitator/`.
[7] Wiklund M., *Lab Chip*, **12** (2012) 2018.
[8] Meng L. *et al.*, *J. Phys. D: Appl. Phys.*, **52** (2019) 273001.
[9] Marrara S. *et al.*, *IEEE Trans. Instrum. Meas.*, **72** (2023) 9600808.
[10] Mohsenvand K. *et al.*, *Sci. Rep.*, **14** (2024) 28.
[11] Dholakia K. *et al.*, *Nat. Rev. Phys.*, **2** (2020) 480.
[12] Tolic-Nørrelykke S. F. *et al.*, *Rev. Sci. Instrum.*, **77** (2006) 103101.
[13] Marzo A. *et al.*, *Nat. Commun.*, **6** (2015) 8661.